Rock and Soil Mechanics

Volume 44 | Issue 3 Article 8

7-21-2023

Centrifugal experimental study on seismic response of bridge pile group foundation in saturated sand field overlain by water

Zhi-xiao YAN
College of Civil Engineering and Transportation, Hebei University of Technology, Tianjin 300401, China

Yu-run LI
College of Civil Engineering and Transportation, Hebei University of Technology, Tianjin 300401, China

Dong-sheng WANG
College of Civil Engineering and Transportation, Hebei University of Technology, Tianjin 300401, China

Yong-zhi WANG
Key Laboratory of Earthquake Engineering and Engineering Vibration, Institute of Engineering Mechanics, China Earthquake Administration, Harbin, Heilongjiang 150080, China

Rock and Soil Mechanics 2023 44(3): 861−872 ISSN 1000−7598
https: //doi.org/10.16285/j.rsm.2022.5967 http://rocksoilmech.researchcommons.org/journal

Centrifugal experimental study on seismic response of bridge pile group foundation in saturated sand field overlain by water

YAN Zhi-xiao[1], LI Yu-run[1], WANG Dong-sheng[1], WANG Yong-zhi[2]

1. College of Civil Engineering and Transportation, Hebei University of Technology, Tianjin 300401, China

2. Key Laboratory of Earthquake Engineering and Engineering Vibration, Institute of Engineering Mechanics, China Earthquake Administration, Harbin, Heilongjiang 150080, China

Abstract: In order to explore the dynamic interaction of the soil−pile group foundation−bridge structure system in saturated sand field overlain by water, a physical similarity model of the vertical (inclined) pile group foundation−bridge structure was designed and manufactured. Centrifuge shaking table tests with seismic wave inputs of different ground motion intensities and characteristics were conducted. The dynamic characteristic indices of pile group foundation−bridge structure were analyzed, and the development of excess pore water pressure in the saturated sand foundation overlain by water and the dynamic response of pile−soil interaction were also investigated. The results indicated that the presence of overlying water had slight influence on the basic cycle and damping of the foundation soil−bridge structure system, but caused a 20% increase in the vibration amplitude of the vertical pile group foundation−bridge structure system and a 10% decrease in the vibration amplitude of the inclined pile group foundation−bridge structure system. The damping ratio of the inclined pile group foundation model was twice as high as that of the vertical pile group foundation model. The overlying water caused the saturated sand foundation to change from a larger liquefaction depth under low-frequency vibration to a larger liquefaction depth under high-frequency vibration. Meanwhile, it promoted the development of excess pore water pressure under small earthquakes and vice versa under strong earthquakes. Furthermore, the overlying water would lead to increases in the dynamic response of the bridge superstructure and the pile bending moment. This study could provide an essential reference for the seismic design of bridge engineering in the sand field overlain by water.

Keywords: bridge engineering; seismic performance; centrifuge shaking table test; saturated sand field overlain by water; pile group foundation

1 Introduction

In recent years, pile group foundation has been widely used for river-, lake- and sea-crossing bridge projects[1]. The effective interaction design of overlying water and soil−pile foundation−superstructure is the guarantee for the smooth and stable operation of finely designed bridge superstructures. However, the structural damage of bridges due to foundation liquefaction under seismic loading is still one of the major disasters that bridges are facing at present. For example, the earthquake damage investigations of the Maduo earthquake in May 2021 and the Menyuan earthquake in January 2022 in Qinghai Province, China and the surrounding areas of the earthquake site[2], which causes a severe seismic hazard to several highway and railway bridges. Therefore, studying the dynamic response of soil−pile group−bridge structure interaction in the saturated sand field overlain by water is urgently needed for earthquake disaster mitigation of bridges.

At present, numerous scholars have extensively investigated the interaction between soil−pile foundation−superstructure under seismic loading. For example, Lombardi et al.[3−4] studied the modal parameters of the pile-supported structures during foundation liquefaction. They found that the natural frequency of the pile-supported structures was significantly reduced after the liquefaction of foundation and the structure damping ratio increased to more than 20%. Hui et al.[5] considered the seismic randomness and the cognition uncertainty for a multi-span pile-supported bridge system in liquefiable soil and combined with the uncertainty of the seismic hazard curve to derive the analytical expression of the seismic hazard curve for performance indices. Huang et al.[6] carried out pseudo-static tests under low-frequency cyclic loading to study the interaction between integral abutment−H-shaped steel pile−soil, and the proposed polynomial fitting method and the Huang−Lin method were found to be able to calculate the bending moment and shear force accurately during the integral abutment−pile−soil interaction. Liu et al.[7−8] investigated the liquefiable soil−pile interaction

Received: 24 June 2022 Accepted: 18 September 2022
This work was supported by the National Natural Science Foundation of China (51778207), the Graduate Student Innovation Ability Training Project of Hebei Education Department (CXZZBS2022038) and the Scientific Research Fund of Institute of Engineering Mechanics, China Earthquake Administration (2021D02).
First author: YAN Zhi-xiao, male, born in 1995, PhD candidate, focusing on the research of soil dynamics and pile foundation seismic design.
E-mail: yzxupup@163.com
Corresponding author: LI Yu-run, male, born in 1978, PhD, Professor, Doctoral supervisor, mainly engaged in the research and teaching of geotechnical engineering and foundation engineering. E-mail: iemlyr7888@hebut.edu.cn

under horizontal and vertical vibrations by centrifuge tests, and proved that the dynamic vertical total stress increment was mainly borne by the excess pore water pressure and had no significant effect on the pile bending moment. Li et al.[9] and Yan et al.[10] carried out 2×2 vertical pile group centrifuge tests on saturated sand fields and established a coupled static-dynamic nonlinear finite element model to investigate the acceleration response of foundation liquefaction and distribution characteristics of pile bending moment. Su et al.[11] conducted pile group shaking table tests in the liquefiable field with a medium dense sand layer to compare the dynamic responses of the pile and soil and evaluated the resilience characteristics of the structure. Zhang et al.[12] conducted a series of shaking table tests to investigate the dynamic interaction of soil-frame structures with different natural frequencies, and evaluated the variation of natural frequencies and damping ratios of the soil and structure with the intensity of seismic loading for different soil conditions. Xu et al.[13] investigated the dynamic response and soil−structure interaction of pile foundation−flexible structure on the liquefiable, non-liquefiable and rigid foundations. Feng et al.[14] studied the dynamic response and *p-y* curve of pile−soil interaction for the pile group in the liquefiable site under strong earthquakes based on shaking table tests and the Haiwen Bridge project, and analyzed the differences in dynamic time-history response of large-diameter deep single pile and pile group foundations under strong earthquakes[15]. In addition, several scholars analyzed the seismic performance of nonlinear foundation soil−pile foundation−bridge structures under multi-hazard conditions such as earthquake and flood scouring by means of simplified numerical models[16−19], simplified theoretical models[20−24], and physical model tests[22]. For example, Wang et al.[23] proposed a brittleness-based *tornado diagram* method to assess the sensitivity of bridge structure and soil parameters, and conducted the shaking table tests on bridge pile foundations built at non-liquefiable and liquefiable sites[24] to compare the different failure mechanisms of piles at the two sites and evaluate the pile group effect. It was noted that the pile group effect was significant in non-liquefiable soils, while it was relatively negligible in liquefiable soils.

In summary, scholars have made abundant research results in the study of foundation soil−pile foundation−superstructure interaction. However, the influence of overlying water in the field of bridge projects across rivers, lakes and seas has been rarely reported. Therefore, based on the research results in the literature, this paper carried out the study on the dynamic response of the vertical (inclined) pile group foundation−bridge superstructure system in the saturated sand field overlain by water through large-scale centrifuge shaking table model tests to understand the influence of overlying water on the development of excess pore water in the foundation soil and the response of acceleration. The mechanical characteristics of the pile foundation and the dynamic response of the bridge superstructure were analyzed to reveal the influence of overlying water on the seismic performance of a vertical (inclined) pile group foundation−bridge structure system in the saturated sand field and to provide a reference basis for the seismic design of bridge structures.

2 Experimental set-up

2.1 Test equipment

The centrifuge test was conducted using the large-scale dynamic geotechnical centrifuge test system DCIEM-30-400 at the Huixian Comprehensive Laboratory of Earthquake Engineering, Institute of Engineering Mechanics, China Earthquake Administration (CEA)[25], as shown in Fig. 1(a). The key performance indices of the large-scale geotechnical centrifuge system DCIEM-30-400[26] are as follows: the effective radius of the centrifuge body is 5.0 m, the effective maximum centrifugal acceleration is 100*g*, the maximum mass limit is 3 000 kg, the number of dynamic data collection channels is 168, and the effective basket clearance is 1.6 m (length) ×1.0 m (width)×1.8 m (height). The key performance indices of the horizontal one-way shaking table carried in the centrifuge system are as follows: the maximum vibration acceleration is 30*g*, the maximum vibration speed is 1 m /s, the maximum vibration displacement is ±0.015 m, the effective vibration bandwidth is 10−300 Hz, and the maximum vibration load is 1 500 kg. A laminar shear model box compatible with the centrifuge testing system was used in the test, and its dimensions are 1.20 m (length)×0.50 m (width)×0.65 m (height). The horizontal one-way shaking table and the compatible shear model box are shown in Fig. 1(b).

2.2 Test model

The prototype of the field test was a flooded land field containing a deep saturated sand layer overlain by periodic water, and the thickness of the saturated sand layer was about 15 m. The bridge pile foundation was an end-bearing pile, which passed through the saturated sand layer and embedded on the underlying hard stratum. Considering the actual site condition of the bridge, the foundation soil in this test was Tianjin river sand, whose physico-mechanical parameters are listed in Table 1 and its particle size distribution curve is shown in Fig. 2. In order to ensure the degree of saturation of the saturated

(a) Centrifuge main part (b) Centrifuge basket

Fig. 1 Centrifuge shaking table system DCIEM-30-400

Table 1 Basic physico-mechanical parameters of Tianjin fine sand

Physico-mechanical parameter	G_s	D_{60}/m	C_u	C_c	ρ_{dmax} /(kg • m^{-3})	ρ_{dmin} /(kg • m^{-3})
Tianjin fine sand	2.641	0.000 185	1.7	0.96	1 696	1 482

Note: G_s is the specific gravity; D_{60} is the constrained particle size; C_u is the coefficient of uniformity; C_c is the coefficient of curvature; and ρ_{dmax} and ρ_{dmin} are the maximum and minimum dry densities.

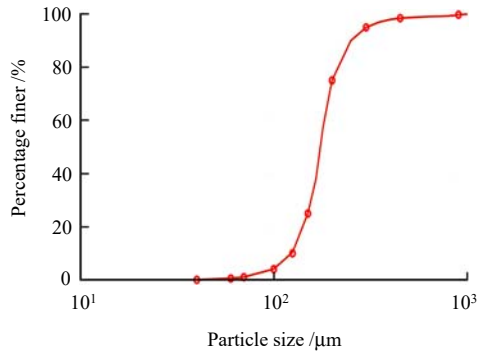

Fig. 2 Particle size distribution curve for Tianjin fine sand

sand foundation, the preparation was divided into two steps. In the first step, the air pluviation method was used to prepare the dry sand foundation, and in the second step, the dry sand foundation was placed in a vacuum environment and fully saturated by hydroxypropyl methylcellulose polymer solution with a viscosity of 50 mPa·s.

The pile group foundation−bridge superstructure test model was based on the design of a multi-span continuous beam bridge, as shown in Fig. 3. The mass of the left and right upper half span bridge plates of the test prototype pier was 563.6 t, the mass of the pile cap of the pile group foundation was 198.4 t, the height of the bridge pier was 10 m, and the 2×2 pile group foundation was symmetrically arranged with a diameter of 1.0 m and flexural stiffness of 1 995.8 MN·m^2. The main control parameters of the test model design included the flexural rigidity of the pile, the natural frequency of the structure, and the mass ratio of the superstructure to the pile cap, considering the kinematic and inertial effects of the superstructure in the seismic analysis of bridges. The model was an elevated pile cap foundation, which was regarded as a two-degree-of-freedom system with the 1st natural period of 0.016 28 s and the 2nd natural period of 0.069 30 s. The mass ratio of the pile cap to the superstructure of the model was 0.35. Based on the performance of the large-scale geotechnical centrifuge test system DCIEM-30-400 and its supporting equipment parameters, the ratio of similitude for this test was determined to be 50. The parameters of the test model were calculated according to the ratio of similitude as shown in Table 2, and the pile in the test model was made of No. 6061 aluminum tube with a diameter of 20 mm, a wall thickness of 2 mm and a length of 500 mm. The inclination angle of the inclined pile was 10°, and the inclined direction of the inclined pile group is consistent with the vibration direction. The pile cap was made of solid aluminum block. The pier was made of solid aluminum column with a diameter of 30 mm. The lumped mass was made of solid steel block, as shown in Fig. 3.

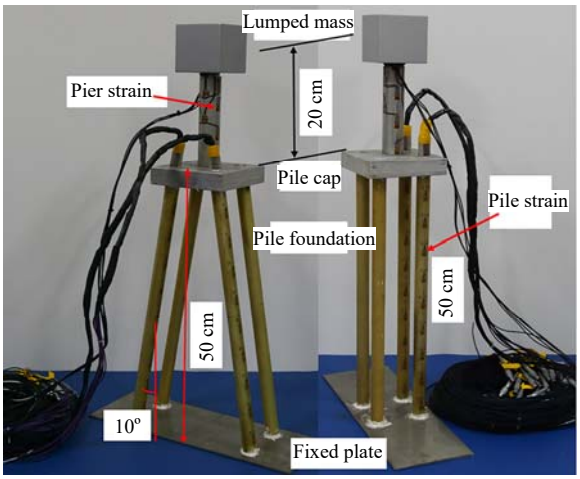

Fig. 3 Test model for vertical (inclined) pile group foundation

Table 2 Test model parameters and ratios of similitude

Part parameter	Lumped mass /kg	Pier		Pile cap		Pile			
		Flexural rigidity /(MN • m^2)	Height /m	Mass /kg	Size /m	Flexural rigidity /(MN • m^2)	Diameter /m	Length /m	Young's modulus /GPa
Prototype	563 750	17 138.1	10.0	198 375	7.0×7.0×1.5	1 995.8	1.0	25	—
Model	4.51	0.002 742 1	0.2	1.587	0.14×0.14×0.03	0.000 319	0.02	0.5	69.2

Note: The ratios of similitude of each parameter except Young's modulus in the table are 50^3, 50^4, 50, 50^3, 50, 50^4, 50, 50 and —.

2.3 Sensor arrangement

High-precision PCB accelerometers were arranged at the superstructure, pile cap and different embedment depths of the foundation soil in the test. High-precision DSP-II pore pressure sensors, independently developed by the Institute of Engineering Mechanics, CEA, were placed at different embedment depths in the foundation soil[27]. Strain sensors were attached to the pile at equal intervals using a full bridge configuration in order to measure the dynamic response of the bending moment at the axis of the pile. The embedment depths of the pore pressure sensor, accelerometers and strain sensor in each foundation soil layer corresponded to each other, ensuring the reliability of the pile−soil interaction analysis after the test. The sensor arrangement is shown in Fig. 4. In the figure, A1−A9 are the PCB accelerometers, and P1−P5 are the DSP-II pore pressure sensors.

2.4 Test case

The El-Centro and Kobe seismic waves were used in the test. The El-Centro seismic wave is a strong seismic

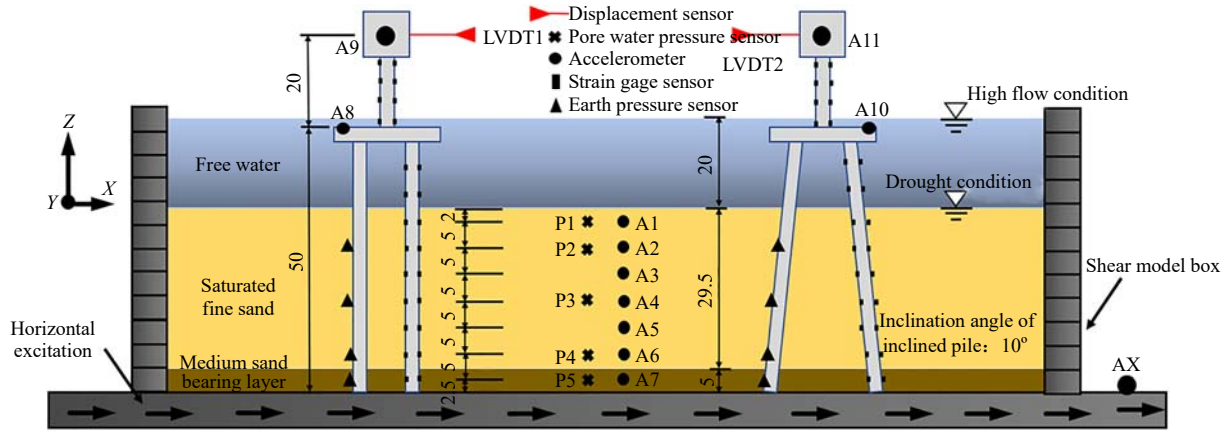

Fig. 4 Sensor arrangement (unit: cm)

wave recorded during the Imperial Valley earthquake in the United State in 1940, which has an original peak acceleration of 0.349*g*, a long strong earthquake duration of up to 26 s, and a dominant period of 0.58 s. The Kobe seismic wave is a strong ground motion measured during the Kobe earthquake in 1995, which is characterized by a short vibration duration and a large content of low-frequency components in the dominant period within 1.06 s. The time history of the ground motion is illustrated in Fig. 5. The test model was also excited by the sweep wave with a peak acceleration of 0.01*g*. The test was divided into two groups: drought condition and high flow condition. In the drought condition, there was no overlying free water on the saturated sand foundation. In the high flow condition, there was free water with a depth of 10 m (prototype) above the saturated sand field. Both groups were excited by the same seven types of ground motion intensities from small to large, and the test cases are tabulated in Table 3.

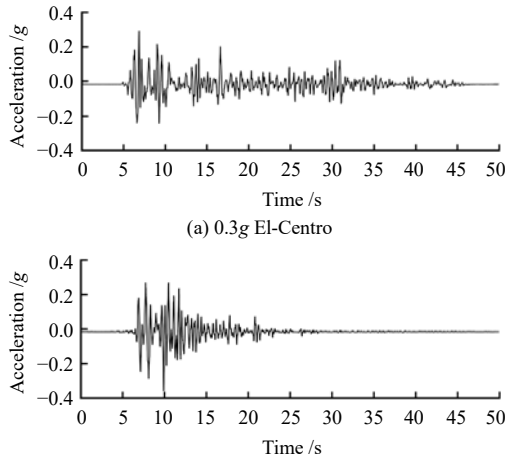

Fig. 5 Time-history curves for 0.30*g* El-Centro and Kobe seismic waves

3 Test results and analysis

3.1 Damping ratio and frequency of foundation−bridge structure system

The test model was first excited by the sweep wave

to obtain the overall natural characteristics of the foundation soil−bridge structure model under drought and dry flow conditions before formally inputting seismic waves into the test model. The fast Fourier transform was used for the acceleration response of the upper lumped mass block. The Fourier transform aimed to transform the obtained time domain acceleration response into the frequency domain-amplitude response. The spectral characteristics of the foundation soil−bridge structure system could be clarified after the Fourier transform. It was difficult to determine the data corresponding to the amplitude peak point merely based on the Fourier transform. Hence, a weighted linear regression function was introduced to treat the acceleration Fourier transform, and the spectral characteristics of the foundation soil−bridge superstructure under the drought and high flow conditions are shown in Figs. 6 and 7.

Table 3 Test conditions of different ground motion inputs

Case	Ground motion type	Ground motion peak /*g*
1	sweep wave	0.01
2	El-Centro	0.05
3	Kobe	0.05
4	El-Centro	0.10
5	Kobe	0.10
6	El-Centro	0.30
7	Kobe	0.30

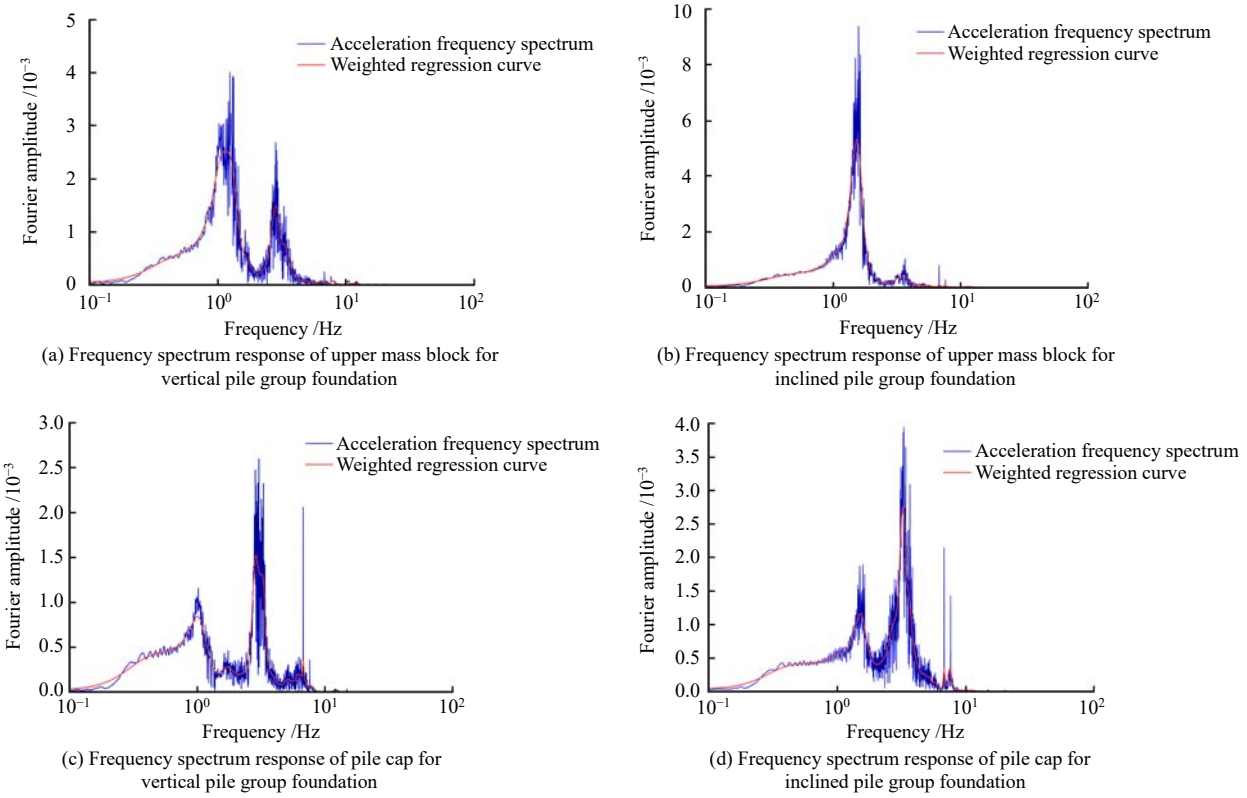

(a) Frequency spectrum response of upper mass block for vertical pile group foundation

(b) Frequency spectrum response of upper mass block for inclined pile group foundation

(c) Frequency spectrum response of pile cap for vertical pile group foundation

(d) Frequency spectrum response of pile cap for inclined pile group foundation

Fig. 6 Fourier transform of structural acceleration response induced by sweep waves in drought conditions

It was found that the 1st and 2nd peak frequency characteristics of the foundation soil−bridge structure system were independent of the overlying water by comparing the high and drought conditions. The frequency characteristics of the peak amplitude of the test model with and without overlying water are shown in Table 4. The presence of overlying water layer obviously affected the vibration amplitude of the test model, the amplitude of the vertical pile group foundation test model in the high flow condition was 20% higher than that in the drought condition, and the amplitude of the inclined pile group foundation test model in the high flow condition was reduced by about 10%. Comparing the spectral characteristics of vertical and inclined pile group foundations under the same condition, it was found that the 2nd peak frequency of the inclined pile group foundation model was larger, the vertical pile group foundation model was closer to the double degree of freedom system, and the spectral characteristics at the superstructure of the inclined pile group foundation model was closer to the single degree of freedom system (SDOF). The reason was due to the fact that the inclined pile in the inclined pile group model was capable of resisting lateral load. The inclined pile, the pile cap and the base plate of the model formed a triangle-like stable structure, thus the lumped mass of the upper overhang was similar to the single degree of freedom system, but the dynamic response amplitude of both the superstructure and the pile cap of the inclined pile group foundation model was larger than that of the vertical pile group foundation. Comparing the spectral

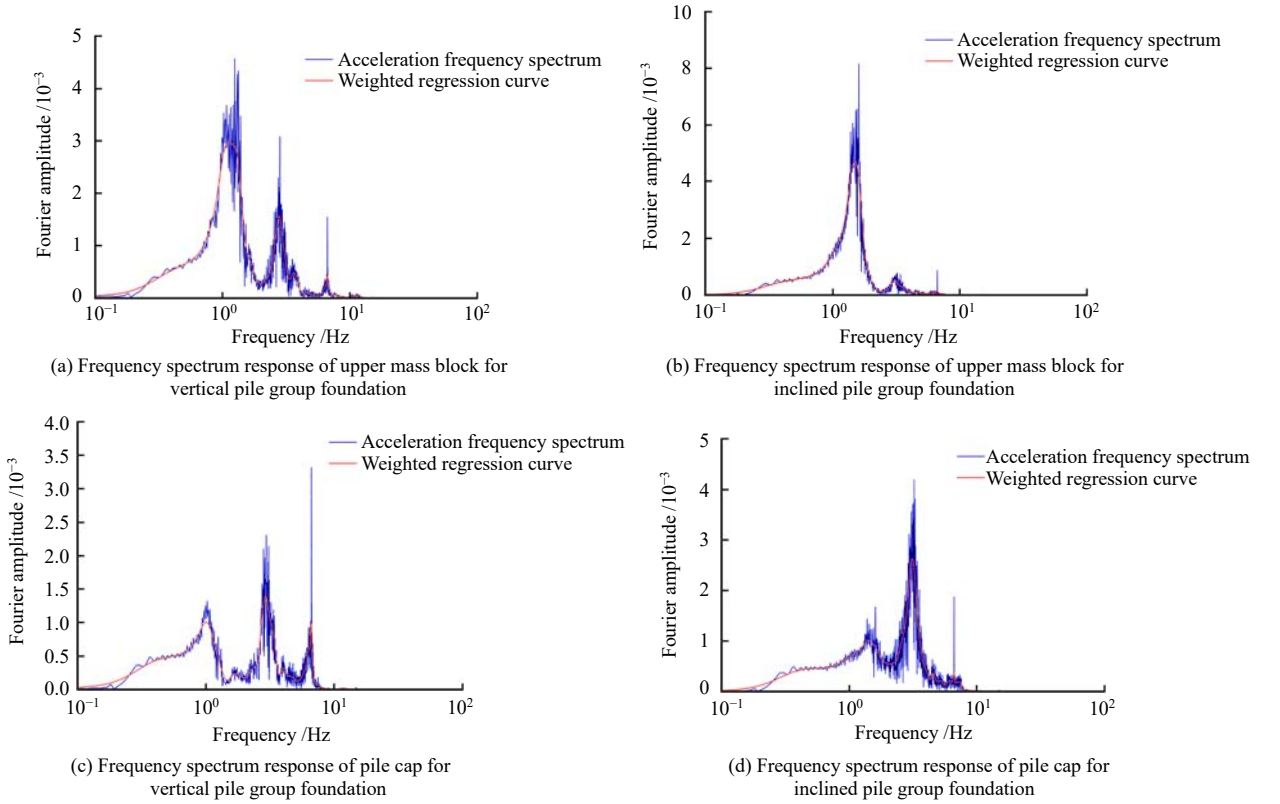

(a) Frequency spectrum response of upper mass block for vertical pile group foundation

(b) Frequency spectrum response of upper mass block for inclined pile group foundation

(c) Frequency spectrum response of pile cap for vertical pile group foundation

(d) Frequency spectrum response of pile cap for inclined pile group foundation

Fig. 7 Fourier transform of structural acceleration response induced by sweep waves in high flow conditions

characteristics at the lumped mass and the pile cap in the same condition, the 1st peak frequency was controlled by the mass at the corresponding position, and the test model was considered as a two degree of freedom system with two modals. The frequency corresponding to the 1st peak amplitude in Fig. 6(a) was controlled by the mass block at the acceleration sampling point. The frequency−amplitude spectral characteristics at this point can be described as the superposition of the 1st and 2nd modals of the test model, and the form of the modals controlled by the upper lumped mass was dominant.

Table 4 Frequency characteristics of foundation soil−bridge structure system (unit: Hz)

Frequency	Drought condition				High flow condition			
	Z_{mass}	X_{mass}	Z_{cap}	X_{cap}	Z_{mass}	X_{mass}	Z_{cap}	X_{cap}
1st peak frequency	1.146	1.537	2.884	3.232	1.117	1.511	2.957	3.149
2nd peak frequency	2.853	3.579	1.010	1.516	2.809	3.106	1.021	1.426

Note: Z_{mass} indicates the location of the upper lumped mass of vertical pile group foundation; Z_{cap} indicates the location of the pile cap of vertical group pile foundation; X_{mass} indicates the location of the upper lumped mass of inclined pile group foundation; and X_{cap} indicates the location of the pile cap of inclined pile group foundation.

The 1st peak amplitude at the upper lumped mass of the foundation soil−bridge structure system under the drought and high flow conditions was obtained as H_m through Figs. 6 and 7. The frequencies corresponding to H_m are the two frequencies f_1 and f_2 corresponding to f_n and $H_m/\sqrt{2}$. The damping ratio ξ of the model was estimated by the half-power bandwidth method. The dominant frequency, dominant period and damping ratio are shown in Table 5, and the damping ratio is calculated as

$$\xi = \frac{f_2 - f_1}{2f_n} \tag{1}$$

It can be seen from Table 5 that the overlying water layer slightly increased the dominant period and damping ratio of the foundation soil−bridge structure system. The damping ratios of the vertical pile group foundation−bridge structure system in the drought and high flow conditions were 2.13 and 1.78 times those of inclined pile group foundation−bridge structure system. The measured dominant frequencies, dominant periods and damping ratios would be used in the later numerical simulation.

Table 5 Frequency and damping characteristics of foundation soil−bridge structure system

Structure	Drought condition			High flow condition		
	Dominant frequency /Hz	Dominant period /s	Damping ratio /%	Dominant frequency /Hz	Dominant period /s	Damping ratio /%
Z	1.146	0.873	19.2	1.117	0.895	20.6
X	1.537	0.651	9.0	1.511	0.662	11.6

Note: Z indicates the vertical pile group foundation−bridge structure and X indicates the inclined pile group foundation−bridge structure.

3.2 Excess pore pressure ratio and acceleration response of saturated sand foundation

The development characteristics of the excess pore pressure ratio at different embedment depths in the foundation soil under the actions of El-Centro and Kobe seismic waves with the peak accelerations of 0.05*g* and 0.30*g* are illustrated in Figs. 8 and 9, respectively. The excess pore pressure ratio r_u is calculated as

$$r_u = \Delta p / \sigma'_v \quad (2)$$

where σ'_v is the effective stress of the overlying soil at the pore water pressure sampling point; and Δp is the dynamic pore water pressure at the sampling point, which is the total pore water pressure recorded by the pore water pressure sensor minus the static pore water pressure at that point. When $r_u \geqslant 1.0$, i.e. the dynamic pore water pressure of foundation soil is greater than or equal to the effective overburden stress of the foundation soil, the foundation soil will lose strength and produce certain mobility, and this phenomenon is called foundation liquefaction. By comparing the cases with peak accelerations of 0.05*g* and 0.30*g*, it can be found that the excess pore pressure ratio reached up to 0.2 in the case with a peak acceleration of 0.05*g* due to the small ground motion intensity, and the foundation soil was not liquefied. When the foundation soil was subjected to the strong ground motion with a peak acceleration of 0.30*g*, the dynamic pore water pressure accumulated rapidly, the excess pore pressure ratio increased quickly and remained near r_u = 1.0 at the ground surface, and the foundation soil was gradually liquefied from shallow to deep. After the end of ground motion, the excess pore pressure ratio started to decrease first in the deep foundation soil. The reason was that the excess pore water between soil particles was gradually discharged from the deep soil layer to the ground surface at the end of ground motion and the effective stress of foundation soil was gradually recovered, thus the excess pore pressure ratio of the ground surface was maintained at 1.0 for a longer time than that at the deep foundation soil. It can be found by comparing the El-Centro and Kobe seismic wave cases with the same peak acceleration that in the case of saturated sand field without overlying water, the development of pore water pressure in foundation soil was faster under the Kobe seismic wave condition containing more low-frequency components, while the pore water pressure in foundation soil developed faster in the El-Centro wave case containing more high-frequency components in the presence of overlying free water. Under the action of seismic waves with small peak acceleration, the overlying water obviously increased the excess pore pressure ratio of the foundation soil. Under the strong ground motion with a peak acceleration of 0.30*g*, the overlying water obviously reduced the excess pore pressure ratio of the foundation soil, which made the liquefaction depth of the foundation soil decrease and generated great negative pore pressure, and this was especially significant in the shallow foundation soil.

Figure 10 shows the acceleration amplification coefficients of the foundation soil at different embedment depths under the action of El-Centro and Kobe seismic waves with a peak acceleration of 0.05*g*. In the figure, "o" indicates the low water condition without overlying water, and "*" indicates the high flow condition with 10 m overlying water in the test prototype. A comparison revealed that the amplification coefficient of the foundation soil decreased from shallow to deep under the seismic wave with a peak acceleration of 0.05*g*. The overall amplification coefficient of the foundation soil under

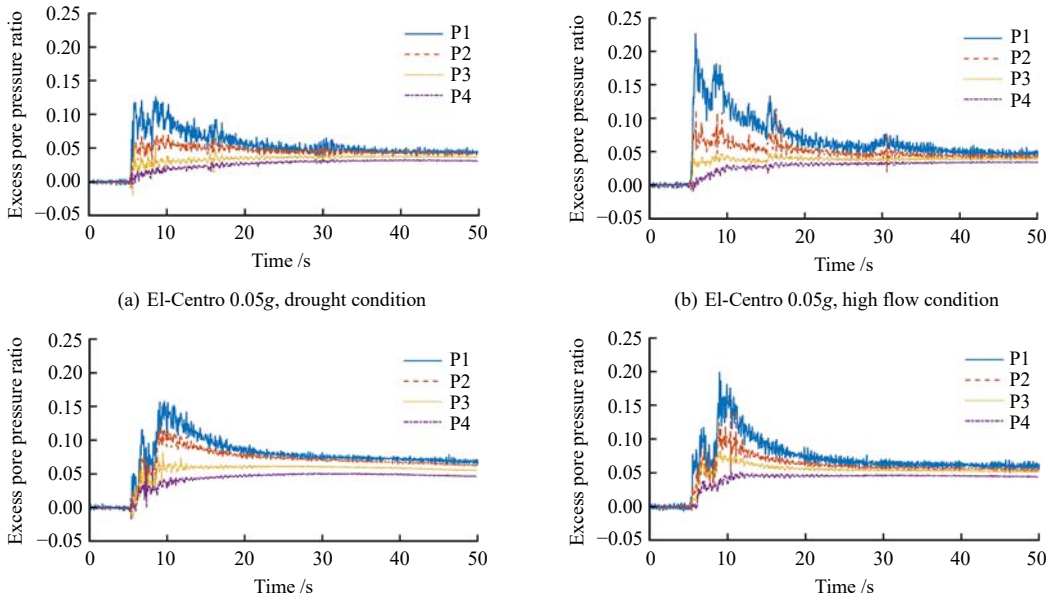

(a) El-Centro 0.05*g*, drought condition

(b) El-Centro 0.05*g*, high flow condition

(c) Kobe 0.05*g*, drought condition

(d) Kobe 0.05*g*, high flow condition

Fig. 8 Development characteristics of excess pore pressure ratio for foundation soil at different depths under the action of El-Centro and Kobe seismic waves with a peak acceleration of 0.05*g*

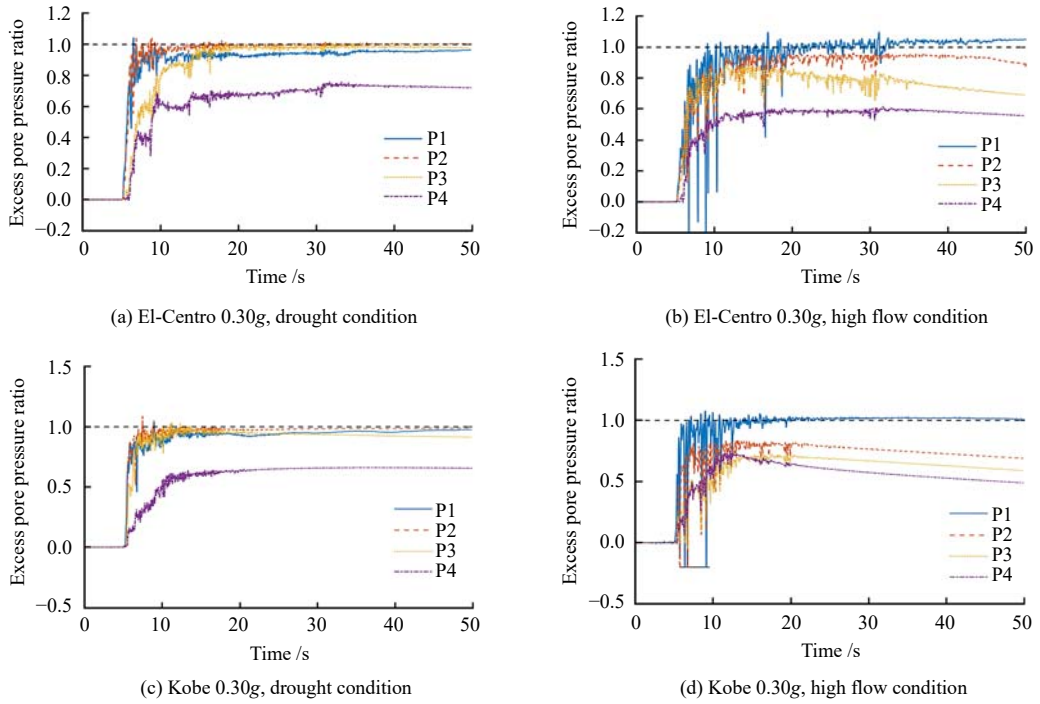

(a) El-Centro 0.30*g*, drought condition (b) El-Centro 0.30*g*, high flow condition

(c) Kobe 0.30*g*, drought condition (d) Kobe 0.30*g*, high flow condition

Fig. 9 Development characteristics of excess pore pressure ratio for foundation soil at different depths under the action of El-Centro and Kobe seismic waves with a peak acceleration of 0.3*g*

the Kobe seismic wave was higher than that under the El-Centro seismic wave. The overlying water effectively reduced the acceleration amplification coefficient of the foundation soil for the El-Centro 0.05*g* case, while it had a weak effect on the 0.05*g* Kobe seismic wave case.

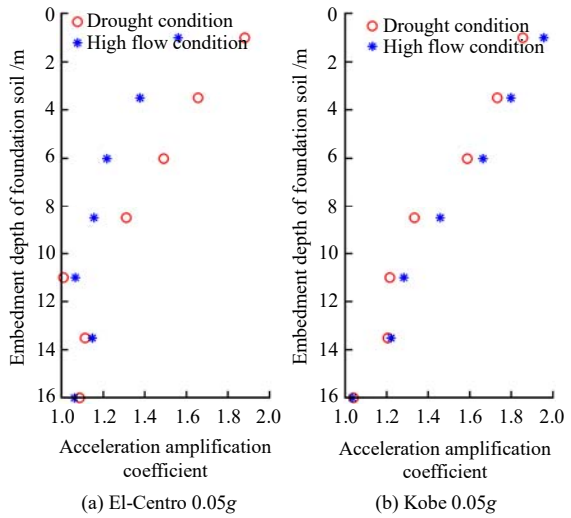

(a) El-Centro 0.05*g* (b) Kobe 0.05*g*

Fig. 10 Acceleration response of soil at different depths induced by 0.05*g* seismic wave

Figure 11 shows the acceleration response of the foundation soil at different depths (A1, A2 and A3) and shaking table input (Ax) for the El-Centro and Kobe seismic waves with a peak acceleration of 0.30*g*, and the time history of the excess pore pressure ratio (P1) corresponding to the shallow foundation soil (A1) is also illustrated. A comparison showed that the liquefaction of the foundation soil was accompanied by the loss of acceleration response. The reason was that due to the liquefaction of the foundation soil, the effective stress was completely lost, the foundation soil lost its strength, and the accelerometer was in a floating state, resulting in signal disappearance. From the analysis of acceleration response at different embedment depths, the shallow liquefaction of the foundation soil occurred first and was accompanied by the process of foundation soil vibration, and the deep foundation soil was difficult to liquefy. The overlying water obviously increased the liquefaction resistance of the foundation soil under the same embedment depth and ground motion conditions.

3.3 Acceleration response of bridge superstructure

Figure 12 provides the amplification trends of acceleration response at the superstructure and the pile cap of the bridge with the vertical (inclined) pile group foundation under the multiple conditions of different peak accelerations of El-Centro and Kobe ground motions and saturated sand field with and without overlying water. In the figure, A_{zmass} indicates the acceleration amplification coefficient at the upper mass block of the vertical pile group model; A_{zcap} indicates the acceleration amplification coefficient at the pile cap of the vertical pile group model; A_{xmass} indicates the acceleration amplification coefficient at the upper mass block of the inclined pile group model; and A_{xcap} indicates the acceleration amplification coefficient at the pile cap of the inclined pile group model. In combination with the comparison of the excess pressure ratio of the foundation soil, it was found that as the input of ground motion intensity increased, the liquefaction of

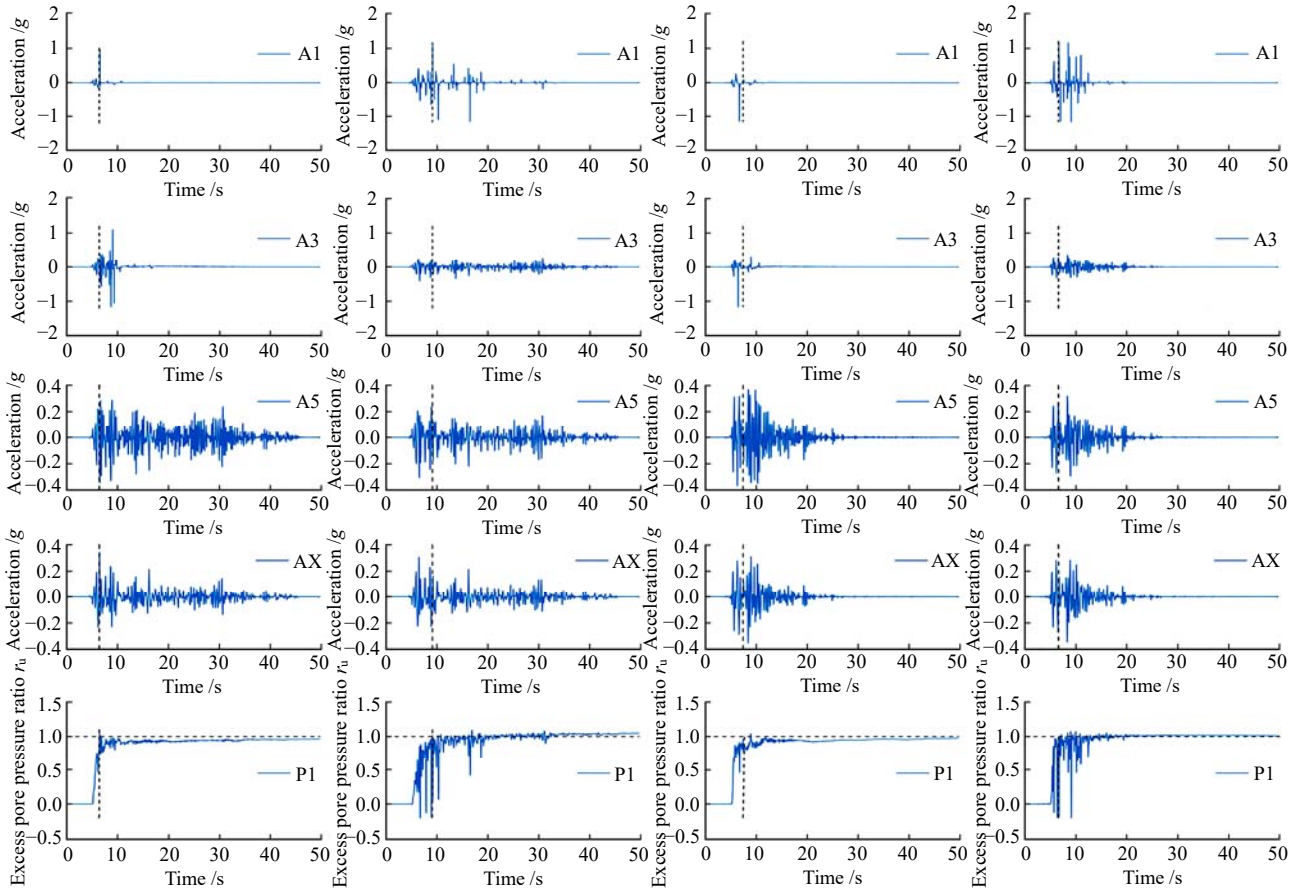

(a) El-Centro 0.30*g*, drought condition (b) El-Centro 0.30*g*, high flow condition (c) Kobe 0.30*g*, drought condition (d) Kobe 0.30*g*, high flow condition

Fig. 11 Acceleration response of foundation soil at different depths induced by seismic wave with a peak acceleration of 0.30*g*

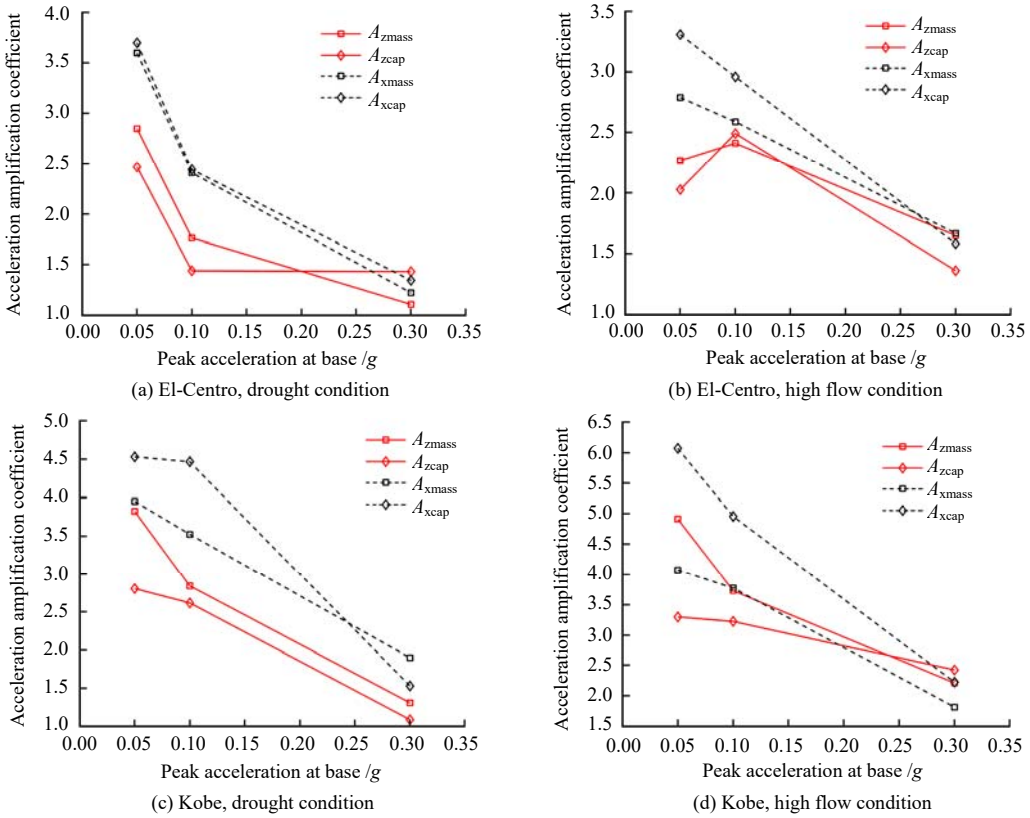

(a) El-Centro, drought condition (b) El-Centro, high flow condition

(c) Kobe, drought condition (d) Kobe, high flow condition

Fig. 12 Influence of ground motion intensity on acceleration response of superstructure

the foundation soil occurred and the liquefaction depth gradually increased. The amplification coefficient of the acceleration response for the pile cap and superstructure of vertical (inclined) pile group foundation reduced gradually,

indicating that the degree of pile−soil interaction was significantly weakened after the foundation soil liquefied and lost its strength. By comparing the dynamic response of different foundation forms, it was found that the amplification coefficient of the acceleration dynamic response at the superstructure and pile cap of vertical pile group foundation was smaller than that of the inclined pile group foundation under the same condition, and the phenomenon was also confirmed by the natural dynamic characteristics of the test model of vertical and inclined pile group foundations in Section 3.1. By comparing the acceleration response of the superstructure and pile cap of the same model, it was found that the acceleration amplification response at the superstructure of the vertical pile group foundation was larger than that at the pile cap when the foundation soil was not liquefied, and the acceleration response at the pile cap was larger than that when the superstructure after the foundation was liquefied. The acceleration response of the inclined pile group foundation at the pile cap was larger than that at the superstructure when the foundation soil was not liquefied, and the acceleration response at the superstructure was greater than that at the pile cap after the liquefaction of foundation soil. By comparing the low and high flow condition, the overlying water effectively increased the acceleration response at the superstructure of the bridge structure and the pile cap. Comparison of the El-Centro and Kobe seismic wave conditions showed that the Kobe ground motion condition containing a large number of low-frequency components led to a greater acceleration response of the bridge structure system with vertical (inclined) pile group foundations at the superstructure and pile cap, indicating that low-frequency strong earthquakes were more likely to threaten the safety of bridges.

3.4 Analysis of pile bending moment

The axial strain gages were evenly arranged at an interval of 5 cm between the pile and the upper pier of the test model, as shown in Fig. 4. The strain gages were symmetrically placed at the same position of the pile and were in a full bridge configuration, in order to measure the strain at the pile axis. The strain signals were collected at 5K frequency to provide data for the analysis of pile bending moment distribution. The pile bending moment calculated by the strain signal is

$$M = \frac{\Delta\varepsilon EI_Z}{y} \tag{3}$$

where M is the cross-sectional bending moment at a point on the pile at a given moment; $\Delta\varepsilon$ is the axis strain signal; E is the pile modulus of elasticity; y is the distance from the cross-sectional strain point to the neutral axis (pile radius); and I_Z is the moment of inertia of the cross-section to the neutral axis.

Figure 13 shows the bending moment envelopes of the vertical and inclined pile group foundations at different water depths under the action of Kobe seismic wave with 0.05g, 0.10g and 0.30g peak accelerations. The bending moment distribution of the vertical and inclined pile group foundations in the drought condition was in the shape of vase. The bending moment at the interface of foundation and soil was the smallest. The connection between the pile and the pile cap were fixed. The bending moment was amplified at the pile cap. As the peak of Kobe ground motion increased, the position of the maximum pile bending moment moved deeper in the foundation soil. This was because with the increase of the peak of ground motion, the liquefaction depth of foundation soil intensified and the constraint of the foundation soil to the pile foundation shifted downward. The bending moment of the inclined pile group foundation in the drought condition showed a broken line variation along the direction of embedment depth, which narrowed at the interface between foundation and soil. The maximum pile bending moment occurred at the embedment depth of about six times the pile diameter in the foundation soil, and the pile bending moment at the deep foundation soil was tiny under small peak accelerations. The reason was that the foundation soil had a strong constraining ability to the pile foundation when the foundation soil was not liquefied or the liquefaction depth was shallow. Because the pile was inclined and had an inclination angle, the bottom of the pile was more subjected to axial tension and pressure from the upper part and sustained less bending and shear forces. Compared with the small peak conditions, the pile bending moment of the inclined pile group foundation increased significantly under the large peak acceleration due to the increase of liquefaction depth of foundation soil. Comparing the pile bending moment of the vertical and inclined pile group foundations, it was found that the pile bending moment of the inclined pile group was large as a whole. The comparison between the high flow condition and the drought condition indicated that there was an overall increase in the pile bending moment by about 20% under the interaction of the overlying water and pile foundation during the ground motion input. Due to the presence of overlying water, there was no liquefaction in the deep foundation soil with the input of Kobe seismic wave with a peak acceleration of 0.30g in the high flow condition, and the pile bending moment of the inclined pile group foundation decreased evidently in the high flow condition compared with that in the drought condition. Through the analysis, it was found that the bearing capacity design of bridge pile foundations in the fields with saturated sand overlain by water should be improved to provide sufficient lateral dynamic bearing capacity for bridge structures after the overlying water deepened in the fields during flood and tide seasons.

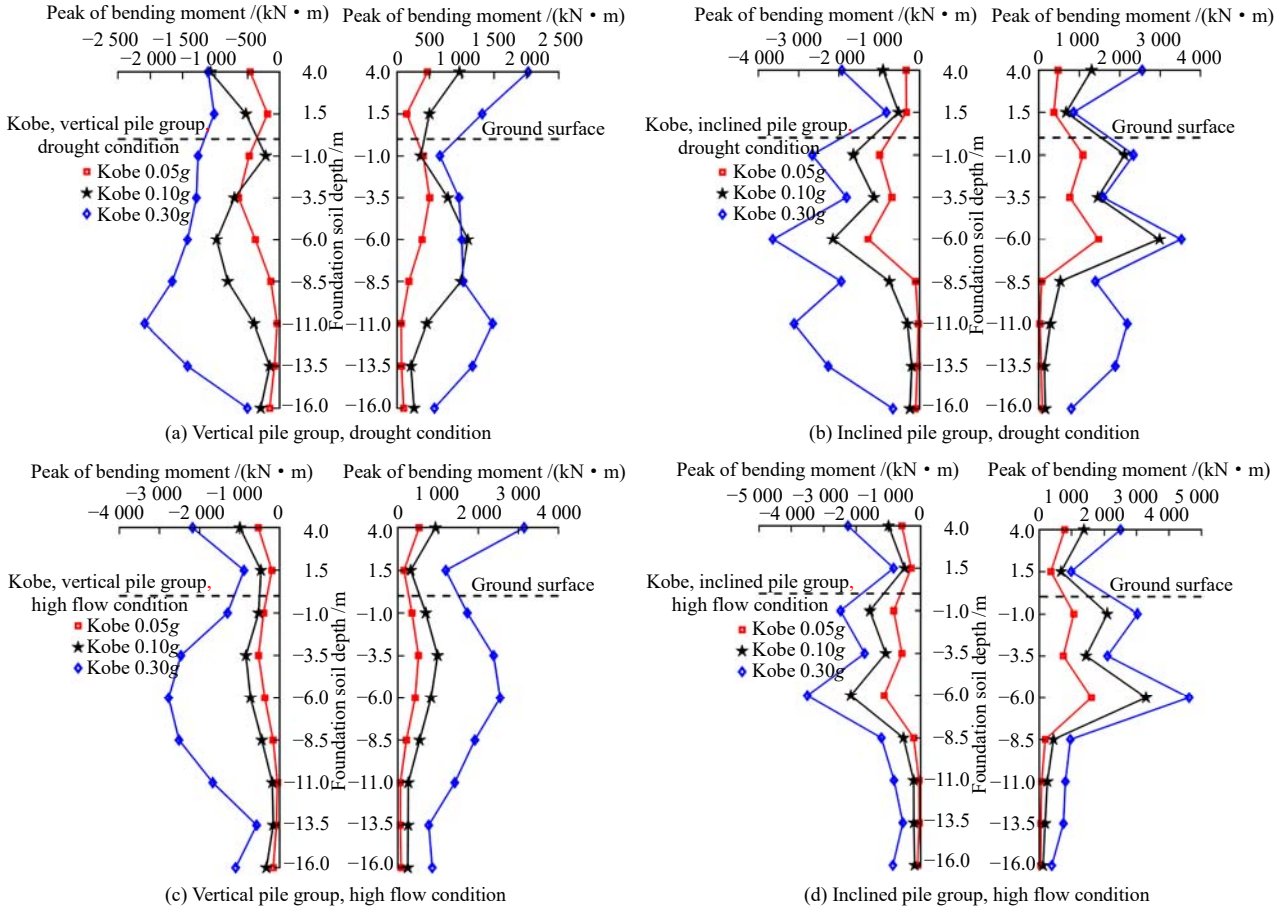

Fig. 13 Pile bending moment envelopes under Kobe seismic wave input

4 Conclusions

Through the centrifuge shaking table test of soil−pile group foundation−bridge superstructure interaction in the saturated sand field overlain by water, the effects of overlying water, ground motion intensity and ground motion characteristic on the development of pore water pressure and the response of acceleration of the foundation soil were explored, and the dynamic responses under seismic loading of the pile bending moment distribution, pile cap and bridge superstructure were analyzed. The conclusions are drawn as follows:

(1) The water above the saturated sand field had little effect on the fundamental period and damping of the foundation soil−bridge structure system, but it can increase the vibration amplitude of the acceleration response for the bridge structure with vertical pile foundations by 20% and decrease the vibration amplitude of the acceleration response for the bridge structure with inclined pile foundations by 10%. The bridge structure model with the inclined pile group foundation had a larger damping ratio than that with the vertical pile group foundation. The damping ratio of the bridge structure model with the inclined pile group foundation was about twice as large as the bridge structure model with the vertical group pile foundation.

(2) The liquefaction depth of saturated sand foundation was more affected by high-frequency vibration than low-frequency vibration due to the presence of overlying water. Compared with the saturated sand field without overlying water, the overlying water promoted the development of excess pore pressure ratio in the saturated sand foundation under small earthquakes and had a suppressive effect under strong earthquakes.

(3) The saturated sand foundation was not liquefied in the small earthquake condition, and the acceleration amplification coefficient reduced gradually as the embedment depth increased from shallow to deep. For the foundation liquefaction under the strong earthquake condition, the shallow foundation soil was liquefied and the acceleration response disappeared. The deep foundation soil was not liquefied and the acceleration response of the input ground motion presented an amplification characteristic.

(4) Compared with the inclined pile group foundation, the dynamic responses of the superstructure and pile cap of the vertical pile group foundation were small. The presence of overlying water significantly increased the dynamic response of the bridge superstructure and pile cap. With the increase of ground motion intensity, the liquefaction depth of the foundation soil increased and the ground motion amplification coefficient at the bridge superstructure and pile cap reduced rapidly. Low-frequency strong earthquake was more likely to induce the failure of the bridge superstructure and pile cap in saturated sand

fields.

(5) The pile bending moment of the vertical pile group was smaller than that of the inclined pile group. The most unfavorable condition of the vertical and inclined pile groups was found at the embedment depth of about six times the pile diameter in the foundation soil. The presence of overlying water could increase the cross-sectional bending moment of pile foundations in the saturated sand foundation, and the bearing capacity of pile foundations in the saturated sand fields overlain by water should be enhanced during the seismic design.

References

[1] WANG Xiao-wei, HE Zhong-ying, YE Ai-jun. Experimental study on seismic failure mechanism of elevated pile-cap foundation for bridge structures[J]. Journal of Tongji University (Natural Science), 2014, 42(9): 1313−1320.

[2] LIU Wei, ZHANG Hao-yu, HUANG Yong, et al. Investigation and discussion of the building seismic damage after Qinghai Maduo Ms 7.4 earthquake in 2021[J]. World Earthquake Engineering, 2021, 37(3): 57−64.

[3] LOMBARDI D, BHATTACHARYA S. Modal analysis of pile-supported structures during seismic liquefaction[J]. Earthquake Engineering and Structural Dynamics, 2014, 43(1): 119−138.

[4] LOMBARDI D, BHATTACHARYA S. Evaluation of seismic performance of pile-supported models in liquefiable soils[J]. Earthquake Engineering and Structural Dynamics, 2016, 45(6): 1−24.

[5] HUI Shu-qing, TANG Liang, LING Xian-zhang. Performance-based seismic response of the multi-span pile-supported bridge system in liquefiable soil[J]. World Earthquake Engineering, 2022, 38(1): 158−166.

[6] HUANG Fu-yun, ZHAGN Feng, SHAN Yu-lin. Calculation method of internal force of integral abutment pile foundation-soil interaction[J]. China Journal of Highway and Transport, 2021, 34(6): 69−79.

[7] LIU X, WANG R, ZHANG J M. Centrifuge shaking table tests on 4×4 pile groups in liquefiable ground[J]. Acta Geotechnica, 2018, 13(6): 5−18.

[8] LIU Xing, WANG Rui, ZHANG Jian-min. Seismic response analysis of pile groups in liquefiable foundations[J]. Chinese Journal of Geotechnical Engineering, 2015, 37(12): 2326−2331.

[9] LI Yu-run, YAN Zhi-xiao, ZHANG Jian. Centrifugal shaking table test and numerical simulation of dynamic responses of straight pile group in saturated sand[J]. Chinese Journal of Rock Mechanics and Engineering, 2020, 39(6): 1252−1264.

[10] YAN Zhi-xiao, LI Yu-run, ZHANG Jian. Seismic response characteristics of straight group piles and soil in saturated sand[J]. Journal of Vibration and Shock, 2020, 39(18): 44−53.

[11] SU L, TANG L, LING X Z, et al. Responses of reinforced concrete pile group in two-layered liquefied soils-shake-table investigations[J]. Journal of Zhejiang University-Science A(Applied Physics & Engineering), 2015, 16(2): 93−104.

[12] ZHANG Z Y, WEI H Y, QIN X. Experimental study on damping characteristics of soil-structure interaction system based on shaking table test[J]. Soil Dynamics and Earthquake Engineering, 2017, 98: 183−190.

[13] XU C S, DOU P F, DU X L. Large shaking table tests of pile-supported structures in different ground conditions[J]. Soil Dynamics and Earthquake Engineering, 2020, 139: 106307.

[14] FENG Zhong-ju, MENG Ying-ying, ZHANG Cong, et al. Dynamic response and *p-y* curve of pile groups in liquefaction site under strong earthquake[J]. Rock and Soil Mechanics, 2022, 43(5): 1289−1298.

[15] ZHANG Cong, FENG Zhong-ju, MENG Ying-ying, et al. Shaking table test on the difference of dynamic time-history response between single pile and pile group foundation[J]. Rock and Soil Mechanics, 2022, 43(5): 1326−1334.

[16] WANG Xiao-wei, LI Chuang, YE Ai-jun, et al. Seismic demand analysis of simply supported girder bridge in liquefied or non-liquefied ground[J]. China Journal of Highway and Transport, 2016, 29(4): 85−95.

[17] GUO X, WU Y, GUO Y. Time-dependent seismic fragility analysis of bridge systems under scour hazard and earthquake loads[J]. Engineering Structures, 2016, 121: 52−60.

[18] GUO X, BADRODDIN M, CHEN Z. Scour-dependent empirical fragility modelling of bridge structures under earthquakes[J]. Advances in Structural Engineering, 2018, 21(6): 1384−1398.

[19] FIOKLOU A, ALIPOUR A. Significance of non-uniform scour on the seismic performance of bridges[J]. Structure and Infrastructure Engineering, 2019, 15(6): 822−836.

[20] SONG S T, WANG C Y, HUANG W H. Earthquake damage potential and critical scour depth of bridges exposed to flood and seismic hazards under lateral seismic loads[J]. Earthquake Engineering and Engineering Vibration, 2015, 14(4): 579−594.

[21] XU Y, SHANG Y, YE A J. Dynamic interaction between bridge pier and its large pile foundation considering earthquake and scour depths[J]. Advances in Structural Engineering, 2016, 19(9): 1390−1402.

[22] LIANG F Y, LIANG X, ZHANG H, et al. Seismic response from centrifuge model tests of a scoured bridge with a pile- group foundation[J]. Journal of Bridge Engineering, 2020, 25(8): 04020054.

[23] WANG X W, YE A J, JI B. Fragility-based sensitivity analysis on the seismic performance of pile-group-supported bridges in liquefiable ground undergoing scour potentials[J]. Engineering Structures, 2019, 198: 109427.

[24] WANG X W, YE A J, SHANG Y. Shake-table investigation of scoured RC pile-group-supported bridges in liquefiable and nonliquefiable soils[J]. Earthquake Engineering and Structural Dynamics, 2019, 48(11): 1217−1237.

[25] WANG Yong-zhi. Study on design theory and key technology of large dynamic centrifuge[D]. Harbin: Institute of Engineering Mechanics, China Earthquake Administration, 2013.

[26] WANG Yong-zhi, WANG Ti-qiang, WANG Hai, et al. Geotechnical centrifuge progress and key technologies in China[J]. Journal of Seismological Research, 2020, 43(3): 592−600.

[27] TANG Zhao-guang, WANG Yong-zhi, DUAN Xue-feng, et al. Development and performance evaluation of separable high-frequency response miniature pore water pressure transducer[J]. Chinese Journal of Geotechnical Engineering, 2021, 43(7): 1210−1219.